Single-mode Spontaneous Emission from a Single Quantum Dot in a Three-Dimensional Microcavity

G. S. Solomon,[1,2] M. Pelton,[1] and Y. Yamamoto[1,3]

[1]*Quantum Entanglement Project, ICORP, JST, Edward L. Ginzton Laboratory, Stanford University, Stanford, California 94305-4085*

[2]*Solid State Photonics Laboratory, Stanford University, Stanford, California 94305-4085*

[3]*NTT Basic Research Laboratories, 3-1 Morinosoto-Wakamiya, Atsugi, Karagawa, 243-01, Japan*

(Received 25 October 2000)

The spontaneous emission from an isolated semiconductor quantum dot state has been coupled with high efficiency to a single, polarization-degenerate cavity mode. The InAs quantum dot is epitaxially formed and embedded in a planar epitaxial microcavity, which is processed into a post of submicron diameter. The single quantum dot spontaneous emission lifetime is reduced from the noncavity value of 1.3 ns to 280 ps, resulting in a single-mode spontaneous emission coupling efficiency of 78%.

DOI: 10.1103/PhysRevLett.86.3903 PACS numbers: 78.66.Fd, 42.50.Ct, 42.70.Qs, 68.65.–k

Spontaneous emission of an atom is often thought of as an inherent property of the atom, but is, in fact, a result of the interaction between the atom dipole and the vacuum electromagnetic fields. Therefore, the radiation emitted can be altered by suitably modifying the surrounding vacuum fields with a cavity [1,2]. The radiative transition rate of an atom from an excited, initial state, $|i\rangle$, to a lower energy, final state, $|f\rangle$, depends on the available photon field density of states, $\rho(\upsilon_c)$, at the transition frequency, υ_c. In the weak-coupling regime, where the atomic excitation is irreversibly lost to the field, this rate is conveniently expressed by Fermi's golden rule as $(2\pi/\hbar)\rho(\upsilon_c)|\langle f|H|i\rangle|^2$, where H is the atom-vacuum field dipole interaction Hamiltonian. Thus, by altering $\rho(\upsilon_c)$ the spontaneous emission can be enhanced or suppressed. This can be achieved using an optical cavity which reduces the number of allowed modes, but increases the vacuum field intensity in these resonant modes. The spontaneous emission outside the cavity resonance is suppressed, and the spontaneous emission within the cavity resonance is enhanced. For a localized atom with a negligible linewidth that is on resonance at the antinode of the standing wave, the enhancement factor is $3Q\lambda^3/4\pi^2V$, where Q is the cavity quality factor, λ is the transition wavelength, and V is the cavity mode volume. This has been verified by pioneering experiments in the 1980s using atoms passed through a cavity, which exhibit enhanced and inhibited spontaneous emission [3–6]. Researchers are currently applying this principle, called cavity quantum electrodynamics (QED), to important semiconductor nanostructures [7]; of particular interest are high-efficiency light-emitting diodes for optical communications and single photon sources for quantum cryptography [8,9].

In semiconductor systems, enhanced and inhibited spontaneous emission from quantum well (QW) excitons has been demonstrated using a planar microcavity [10,11]. The microcavity is formed by two distributed-Bragg reflectors (DBRs) separated by a $m\lambda/2$ cavity region, where λ is the wavelength of the light in the material and m is an integer. Because of the one-dimensional confinement of photon fields and excitons, the spontaneous emission rate is only slightly modified. The spontaneous emission coupling coefficient β, defined as the fraction of total spontaneous emission from the source that is captured into the fundamental cavity mode, is less than 1%. The three-dimensional photonic band gap structure has been proposed to increase β close to one [12]. Using lithographic processing or lateral oxidation techniques, three-dimensional post microcavities have shown enhanced spontaneous emission efficiency and could be used to achieve the same goal [13–15]. If β is made close to one, semiconductor devices such as a thresholdless laser [10,11], sub-Poissonian light-emitting diode [16], and single-photon turnstile device [8] could be realized.

Here we demonstrate a semiconductor analog of a single-atom cavity QED experiment, using a single quantum dot (QD) as the artificial atom, which is positioned in a three-dimensional post microcavity and coupled to a single optical mode. The QD features well-separated, discrete energy levels and possesses a large optical matrix element, making possible the efficient cavity QED reduction of spontaneous emission lifetime down to 280 ps. Because all the emission is from a single QD, the integrated spontaneous emission coupling efficiency into a single (polarization-degenerate) spatial mode of the device is nearly ideal, up to 78%.

The QDs and planar microcavity were fabricated monolithically using molecular-beam epitaxy. The nanometer-scale QDs (22 nm in-plane diameter, 4 nm high) were formed from InAs in a GaAs matrix by a strain-induced islanding process, along with an InAs QW region, called the wetting layer [17]. The QW wetting layer is spectrally separated from the QD region. Because of spatial localization, an electron and hole form a three-dimensionally confined exciton which absorbs and emits light at discrete wavelengths, just as do atoms. A uniform ensemble of QDs with no spatial ordering was formed on the growth surface by depositing the equivalent of 2.5 planar monolayers

of InAs, under conditions which give a low QD density of approximately 75 dots/μm^2 [18]. The QDs were subsequently covered by GaAs, which planarizes the growth front. The planar cavity is a wavelength-thick layer of GaAs with 29.5 AlAs/GaAs DBR bottom mirror pairs and 15 top mirror pairs. The structure was patterned into arrays of microposts with cavity diameters ranging from 20 μm to 0.4 μm using electron-beam lithography and anisotropic Cl_2/Ar electron cyclotron resonance dry etching. The sample was etched through the top DBR, the cavity including the QD layer, and a portion of the lower DBR. Since the spontaneous emission enhancement factor is inversely proportional to the mode volume, V, we have utilized a taper in the post, which is a by-product of the etching process, in which the cross-sectional area is minimum in the vicinity of the central optical cavity layer.

A scanning-electron microscope (SEM) image of a particular post is shown in Fig. 1a. The cross-sectional area of the active layer of this device is approximately 0.04 μm^2, which gives close to the minimum possible mode volume, $(\lambda/n)^3$, if we take into account the vertical spread of the field into the top and bottom DBR regions. In this device, there are approximately three QDs in the post. The large refractive-index contrast between the post and the vacuum provides transverse confinement by waveguiding and, in combination with the vertical confinement provided by the DBR cavity, leads to fully three-dimensionally (3D) confined optical modes [19,20].

In Fig. 1b, the photoluminescence (PL) spectrum from such a system is shown, where the emission from a single QD is on resonance with the fundamental cavity mode. The independently measured modified spontaneous emission lifetime of the resonant QD is also shown, along with the theoretically predicted variation of lifetime with respect to the wavelength across the cavity resonance. The spontaneous emission lifetime is measured with a streak camera (and spectrometer attachment) after the pulsed excitation from a 200 fs Ti:Al_2O_3 laser. The details of the theory, which uses no fitting parameters, are described below.

The spontaneous emission from the QD ensemble without a microcavity structure is inhomogeneously broadened over a spectral range of approximately 30 nm, and is composed of sharp, instrumental-resolution limited emission peaks associated with the discrete levels of individual QDs with slightly varying topologies [21]. A planar microcavity has the cavity resonance centered at 932 nm with a cavity quality factor, Q, of 2300. When microposts are formed, the lateral confinement increases the fundamental cavity mode resonance to higher energies (blueshift) and results in discrete modes that increase in separation with decreasing post diameter. In Fig. 2, the fundamental cavity mode energy shift is plotted as a function of the effective post diameter. The post diameters are measured using SEM images. The inset of Fig. 2 is the PL spectrum of a 6 μm diameter microcavity post. The discrete modes are identified as the filtered spontaneous emission of the inhomogeneously broadened QDs. The plotted theoretical mode energies were calculated by factorizing the electromagnetic fields into transverse and longitudinal components. The longitudinal field dependence is calculated using a standard transfer-matrix method, using layer thicknesses known from the crystal growth, and GaAs and AlAs refractive indices [22]. The calculated longitudinal profile gives an effective penetration depth of the cavity mode into the DBRs. In addition, an average refractive index, n_{eff}, is obtained by averaging over the longitudinal direction, using the field intensity as a weighting factor. The effective index is then used in standard waveguide theory to determine the transverse field dependence. Using cylindrical dielectric boundary conditions, a characteristic equation for the modal wave number and corresponding transverse intensity can be solved to provide the blueshift

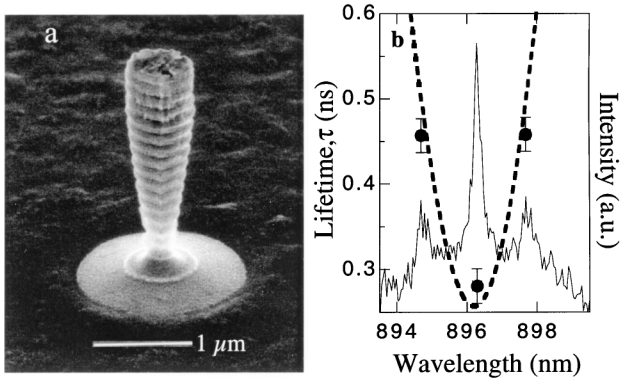

FIG. 1. (a) An SEM image of a typical device, showing the tapered etch and contrasting AlAs and GaAs DBR layers. (b) A photoluminescence (PL) spectrum (solid line) and the spectral dependence of the spontaneous emission lifetime (filled circles: experimental, dashed line: theory) at 4 K with $\leq$0.5 μm cavity diameter showing a single QD resonant with the fundamental cavity mode, and two QDs near the cavity mode edge.

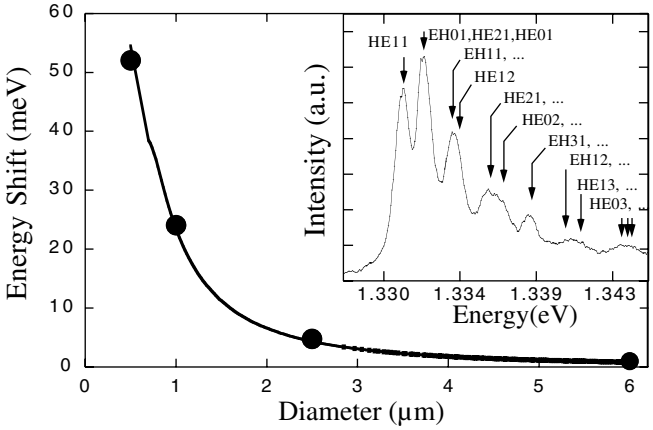

FIG. 2. Measured and calculated energy shifts of the fundamental cavity mode vs post microcavity diameter at 4 K. In the inset, the PL spectrum at 4 K from a 5 μm diameter post microcavity is shown together with the predicted cavity mode eigenenergies (labeled according to transverse waveguide modes).

of the cavity resonance [23]. Quantitative agreement between theoretical and experimental resonance wavelengths is obtained without any free parameters.

Without a cavity, the QDs have a spontaneous emission lifetime of 1.3 ns, and with the planar microcavity this is reduced to 1.1 ns, as shown in Fig. 3a. Here there is a continuous distribution of cavity resonant modes from the cutoff wavelength, $\lambda_c = 2d \simeq 932$ nm to a wavelength corresponding to the stop-band edge. Since the number of modes increases with decreasing wavelength from the cutoff wavelength, λ_c, the spontaneous emission lifetime is continually decreased from the cutoff wavelength to shorter wavelengths. For the 3D post microcavities, the modes are discrete, so that the minimum spontaneous emission lifetime occurs at the center of each mode. This unmistakable mark of the 3D confinement is seen in Fig. 3b for the microcavity with a post diameter of 2.5 μm, where the fundamental modal linewidth is approximately 0.7 nm, and also in Fig. 1b for a post diameter of 0.5 μm, where the fundamental modal linewidth has increased to approximately 3.2 nm. For the 2.5 μm diameter post microcavity, a continuous distribution of QDs emits photons into the single cavity mode. The reduction of spontaneous emission lifetime is largest when the QDs are on resonance, but the modification disappears off resonance, near the mode edge.

To theoretically determine the spontaneous emission lifetime in these microposts we first calculate the effect of leaky modes. While the DBR has a high reflection coefficient only within a limited stop-band angle, we find that the aspect ratio of the smaller posts is large enough that the limited angular stop band of the DBR has no effect. Light incident on the post edges at an angle larger than the critical angle for total internal reflection is also lost as a leaky wave. This critical angle is calculated using the effective refractive index described above. The quality factor Q must be theoretically determined. The dominant mechanism for determining the Q value in our device is diffraction loss through the lower aperture of the post, since it is not completely etched. The field spreads as it penetrates into the lower DBR and on its trip back to the post, and the amount of light that is recaptured by the mode is determined by the overlap of the diffracted field with the transverse mode profile of the post. Independently measured Q values, measured under high pump conditions on several posts, agree with the theory. Although scattering loss due to roughness in the post sidewalls potentially plays a role, it was found that the diffraction loss could nearly completely account for the degradation of Q in our samples. Once the Q and the mode volume are determined, it is straightforward to calculate the spontaneous emission enhancement rate:

$$\frac{\gamma}{\gamma_0} = \frac{Q\lambda_c^3}{2\pi^2 n_{\text{eff}}^3 V_0} \frac{\Delta\lambda_c^2}{\lambda_c^2 + 4(\lambda_e - \lambda_c)^2} + f, \qquad (1)$$

where γ_0 is the experimentally determined emission rate of a QD without a cavity, λ_c is the cavity resonant wavelength, $\Delta\lambda_c$ is the cavity linewidth, $(\lambda_e - \lambda_c)$ is the detuning of the QD emission wavelength from the cavity resonance, and $f\gamma_0$ is the decay rate into the leaky modes, as described above. This value is averaged radially over the post to give an expected decay rate. For posts with diameters of 2 μm or less, $f \approx 0.3$ and increases to 0.9 for 20 μm diameter posts.

In Fig. 3c, the time-dependent spontaneous emission is shown for a single QD in resonance with a 0.5 μm diameter microcavity post. To our knowledge, this is the first time that modified spontaneous emission from a single QD in a three-dimensionally confined cavity has been reported. The rise time ($\approx$50 ps) is determined by the carrier capturing time by the QD and relaxation into the ground state, while the decay time (0.28 ns) is the radiative lifetime. The spontaneous emission lifetime at the center of each fundamental mode is plotted against the post diameter in the inset of Fig. 4, together with the theoretical prediction.

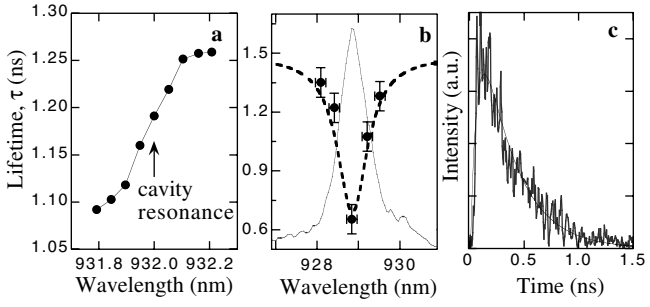

FIG. 3. Spontaneous emission lifetime and photoluminescence intensity vs wavelength for (a) a QD planar microcavity and (b) a QD post microcavity with a diameter of 2.5 μm. In (c) the time-dependent spontaneous emission is shown for a single InAs QD, resonant with the fundamental mode of a 0.5 μm diameter post microcavity.

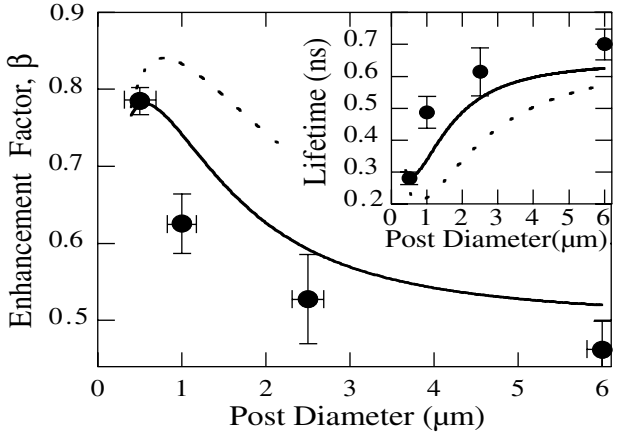

FIG. 4. Spontaneous emission coupling coefficient into the fundamental spatial mode, β, vs the post diameter. β for a single QD in the 0.5 μm diameter post is 0.78. Solid lines indicate the calculated values. In the inset, the experimental and theoretical spontaneous emission lifetimes are plotted as a function of the post diameter. (Solid lines: an average over the post; dashed lines: a single dot at the post center.)

The reduced spontaneous emission lifetime in a small post microcavity is due to the reduced mode volume. This offsets the decrease in Q, which is below 300 in the 0.5 μm diameter post. Using the electric field and mode volume values of these 0.5 μm diameter posts, and the InAs QD dipole strength from the measured free-space radiative lifetime, a cavity Q value of approximately 18 000 will be required to achieve strong coupling with a single QD.

The spontaneous emission coupling coefficient is shown as a function of cavity post diameter in Fig. 4. β is related to the modified spontaneous emission decay rate as $\beta = (\gamma - \gamma_0 - \gamma_c)/\gamma$, where γ is the enhanced spontaneous emission decay rate into the fundamental spatial mode of the cavity, γ_0 is the spontaneous emission decay rate in free space, and γ_c is the fractional spontaneous emission decay rate into the solid angle of the cavity mode in the limit that the mirror reflectivity, $R \rightarrow 0$. Since this solid angle is at most a few degrees in our case, $\gamma_c \ll \gamma_0$. The solid line is the theoretical result with no free parameters. This is in good agreement with the measurement considering only diffractive losses through the bottom DBR mirror have been incorporated, and sidewall scattering, which is difficult to incorporate without fitting parameters, will have some contribution. As well, the factorization of fields into longitudinal and transverse components is inexact, especially for posts with larger diameters. For the smallest microcavity post, β is 0.78. While similar lifetime modifications have been reported in micropost systems, this is the first enhanced β value demonstrated for a single, isolated QD. Systems employing an ensemble of inhomogenously broadened QDs coupled to discrete optical modes [14,15] may have large β and short τ values at the on-resonant condition, but off-resonant β and τ values are small and long, respectively. Averaging over the ensemble of QDs coupled to cavity mode, the overall β and τ values are poor.

Other solid-state structures can be used for increasing β. Whispering gallery mode microdisks have realized a high cavity Q value [24], but isolation of a single QD and efficient light extraction is difficult in such structures [25]. Photonic band-gap structures have also been proposed for achieving high spontaneous emission coupling [12,26], but this has not yet been demonstrated. In this work we have demonstrated that the spontaneous emission lifetime from a single QD can be reduced from 1.3 ns to 280 ps by coupling to the modified vacuum field of a three-dimensional microcavity post. A total of 78% of the emission from the QD state is collected in the discrete fundamental cavity mode, which is normal to the sample. Thus, this work suggests that high quantum efficiency, broad modulation bandwidth nonclassical light sources based on single-mode spontaneous emission will play an important role in quantum communication based on single photons [25,27].

Stanford University provided financial assistance for M. P. The Army Research Office provided partial financial assistance for G. S. S.

[1] E. M. Purcell, Phys. Rev. **69**, 681 (1946).
[2] K. H. Drexhage, *Progress in Optics,* edited by E. Wolfe (North-Holland, Amsterdam, 1974), Vol. XII, pp. 165–232.
[3] P. Goy, J. M. Raimond, M. Gross, and S. Haroche, Phys. Rev. Lett. **50**, 1903 (1983).
[4] G. Gabrielse and H. Dehmelt, Phys. Rev. Lett. **55**, 67 (1985).
[5] R. G. Hulet, E. S. Hilfer, and D. Kleppner, Phys. Rev. Lett. **55**, 2137 (1985).
[6] D. J. Heinzen, J. J. Childs, J. E. Thomas, and M. S. Feld, Phys. Rev. Lett. **58**, 1320 (1987).
[7] *Microcavities and Photonic Bandgaps: Physics and Applications,* edited by J. Rarity and C. Weisbuch (Kluwer, Dordrecht, 1995).
[8] J. Kim, O. Benson, H. Kan, and Y. Yamamoto, Nature (London) **397**, 500 (1999).
[9] A. Imamoğlu, H. Schmidt, G. Woods, and M. Deutsch, Phys. Rev. Lett. **79**, 1467 (1997).
[10] Y. Yamamoto, S. Machida, K. Igeta, and Y. Horikoshi, *Coherence and Quantum Optics,* edited by E. H. Eberly *et al.* (Plenum Press, New York, 1989), Vol. VI, p. 1249.
[11] H. Yokoyama *et al.,* Appl. Phys. Lett. **57**, 2814 (1990).
[12] E. Yablonovitch, Phys. Rev. Lett. **58**, 2059 (1987).
[13] B. Ohnesorge *et al.,* Phys. Rev. B **56**, R4367 (1997).
[14] J. M. Gérard *et al.,* Phys. Rev. Lett. **81**, 1110 (1998).
[15] L. A. Graham, D. L. Huffaker, and D. G. Deppe, Appl. Phys. Lett. **74**, 2408 (1999).
[16] M. Yamanishi, K. Watanabe, N. Jikutani, and M. Ueda, Phys. Rev. Lett. **76**, 3432 (1996).
[17] M. Tabuchi, S. Noda, and A. Sasaki, in *Science and Technology of Mesoscopic Structures,* edited by S. Namba, C. Hamaguchi, and T. Ando (Springer-Verlag, Tokyo, Japan, 1992), p. 379.
[18] G. S. Solomon, J. A. Trezza, and J. S. Harris, Jr., Appl. Phys. Lett. **66**, 991 (1995); **66**, 3161 (1995).
[19] J. M. Gérard *et al.,* Appl. Phys. Lett. **69**, 449 (1996).
[20] J. P. Reithmaier *et al.,* Phys. Rev. Lett. **78**, 378 (1997).
[21] J. Y. Marzin, J. M. Gérard, A. Izrael, D. Barrier, and G. Bastard, Phys. Rev. Lett. **73**, 716 (1994).
[22] G. Bjork, H. Heitmann, and Y. Yamamoto, Phys. Rev. A **47**, 4451 (1993).
[23] G. Panzarini and L. C. Andreani, Phys. Rev. B **60**, 16 799 (1999).
[24] B. Gayral *et al.,* Appl. Phys. Lett. **73**, 1908 (1999).
[25] P. Michler *et al.,* Science **290**, 2282 (2000).
[26] J. Vučković, O. Painter, Y. Xu, A. Yariv, and A. Scherer, IEEE J. Quantum Electron. **35**, 1168 (1999).
[27] C. Santori, M. Pelton, G. S. Solomon, Y. Dale, and Y. Yamamoto, Phys. Rev. Lett. **86**, 1502 (2001).